Radiation Physics and Chemistry 172 (2020) 108820

Contents lists available at ScienceDirect

Radiation Physics and Chemistry

journal homepage: www.elsevier.com/locate/radphyschem

Calculated and experimental response of calcium silicate polycrystalline to high and very-high neutron doses

Carlos D. Gonzales-Lorenzo[a,*], Shigueo Watanabe[a,**], Tássio A. Cavalieri[b], Nilo F. Cano[c,***], T.K. Gundu Rao[a,****], Jose F.D. Chubaci[a], Lucas S. Carmo[b], Carmen C. Bueno[b,*****]

[a] Instituto de Física, Universidade de São Paulo, Rua do Matão, Travessa R, 187, CEP 05508-090, São Paulo, SP, Brazil
[b] Instituto de Pesquisas Energéticas e Nucleares, IPEN-CNEN/SP, Av. Prof. Lineu Prestes, 2242, Cidade Universitária, 05508-000, São Paulo, SP, Brazil
[c] Instituto do Mar, Universidade Federal de São Paulo, Rua. Doutor Carvalho de Mendonça, 144, CEP 11070-100, Santos, SP, Brazil

ARTICLE INFO

Keywords:
$CaSiO_3$
Neutron dosimetry
Thermoluminescence
Monte Carlo
Thermal neutron
(n,γ) reaction

ABSTRACT

In the scope to the discovery of new detectors for high and very-high gamma and neutron radiation dose (mGy-MGy), synthetic polycrystals of $CaSiO_3$ have been produced by the devitrification method in our laboratory. $CaSiO_3$ polycrystals were irradiated with thermal, epithermal and a small fraction of fast neutrons. In the position of irradiation, the thermal neutron flux is about 83% of the total neutron flux and the thermal neutron fluences range from 5.82×10^{13} to 2.97×10^{16} n/cm^2. This thermal neutron reacts with Ca, Si and O through (n,γ) process, all or part of the gamma emitted in this reaction is absorbed by the sample and is responsible for the induction of thermoluminescence (TL). The total energy emitted by the (n,γ) reaction was calculated analytically. Furthermore, Monte Carlo simulations using MCNP5 radiation transport code was carried out to calculate the deposited dose on $CaSiO_3$ by the neutron interaction finding doses ranging from 42 Gy to 21 kGy. $CaSiO_3$ TL glow curves, after radiation exposure from the reactor, display the main prominent TL peak around 234–259 °C and when exposed to gamma radiation (Co-60) it shows the main TL peak around same 234–272 °C.

1. Introduction

Different important reasons have led to the neutron detection investigation, among them, the complexity involved in the neutron interaction with the matter due to accompanying γ-rays that cannot be separated. In this way, studies of neutron interactions with the matter are dealt with separately in thermal, intermediate, fast and monoenergetic neutron (Attix et al., 1969; Douglas, 1978). On the other hand, the detection of neutrons as well as the capacity for distinguishing between neutron and non-neutron radiation, after reactor exposure, using TL detectors have been a great challenge in radiation dosimetry and several works have been devoted for investigating this process in the past (Gambarini et al., 2004; Carrillo et al., 1987; Simpsons, 1965; Vega-Carrillo, 2002; Torres-Cortés et al., 2019; Cavalieri et al., 2019; Obryk et al., 2018; Cerón Ramírez et al., 2016). In a nuclear reactor, the neutron field comes accompanied mostly by gamma radiation. However, other different types of particles such as electrons, photons, protons and also heavy-charged particles can be also emitted (Carrillo et al., 1987; Obryk et al., 2018). For instance, the TLD-600 (^{6}LiF enriched, with 95.6% ^{6}Li) is sensitive to both neutron and gamma, while TLD-700 (^{7}LiF enriched, with 99.9% ^{7}Li) is not responsive to thermal neutrons. Thus, in a mixed radiation field of gamma and thermal neutrons, both TLDs can be used with TLD-700 giving the gamma component and the other detector to be used to calculate the thermal neutron response (Vega-Carrillo, 2002; Carrillo et al., 1987; Cameron et al., 1968). Furthermore, computational tools using the Monte Carlo method were used by some authors to estimate the deposited dose on TL detectors (Cavalieri et al., 2013; Fernandes et al., 2004). On the other hand, Kortov and Ustyantsev (2013) have mentioned some examples of the most sensitive TL dosimeters for low doses as well as various luminescence materials which can be used for high-dose detector creation, among them, the polycrystalline LiF:Mg, Cu, P

* Corresponding authors.
** Corresponding authors.
*** Corresponding authors.
**** Corresponding author.
***** Corresponding author.
E-mail addresses: clorenzo@if.usp.br (C.D. Gonzales-Lorenzo), watanabe@if.usp.br (S. Watanabe), tassio.cavalieri@usp.br (T.A. Cavalieri), nilo.cano@unifesp.br (N.F. Cano), ccbueno@ipen.br (C.C. Bueno).

https://doi.org/10.1016/j.radphyschem.2020.108820
Received 25 July 2019; Received in revised form 15 February 2020; Accepted 1 March 2020
Available online 03 March 2020
0969-806X/ © 2020 Elsevier Ltd. All rights reserved.

detectors, CaF_2, α-Al_2O_3:C, and Brazilian minerals. In this way, several synthetic and natural silicates have shown to be very sensitive for low gamma dose (mGy) and as well for high dose in the order of kGy (Obryk et al., 2011; Watanabe et al., 2015; Gonzales-Lorenzo et al., 2018).

Calcium silicate ($CaSiO_3$) also named as wollastonite is a known material by its different uses in industries of glass, cement, bricks, among others. Wollastonite $CaSiO_3$ exists in three main structural modifications. The stable phase is called pseudowollastonite or β-$CaSiO_3$. It is the high-temperature polymorph and exists above 1150 °C. Secondly, the low-temperature polymorph has two different structures viz., the triclinic wollastonite (1T) and the monoclinic wollastonite (2M), both exist below 1150 °C. This mineral has a type of infinite-chain in the structure, with three SiO_4 tetrahedra in the repeat unit, arranged parallel to *y*-axis (Deer et al., 1992; Hesse, 1984). Souza et al. (2006) performed a dosimetric characterization of natural wollastonite from Minas Gerais, Brazil using a ^{60}Co source; where this mineral has shown a linear behavior of the TL response as a function of absorbed dose. Furthermore, Kulkarni et al. (2011) have studied the TL properties of synthetic nanocrystalline wollastonite.

Polycrystals based on silicates, such as calcium silicate $CaSiO_3$, have shown a high temperature, good stability, and a broad dosimetric peak, when irradiated with high gamma radiation dose, of the order of kGy -MGy, and when irradiated with high neutron fluence, of the order of 10^{13}-10^{16} n/cm^2 (Gonzales-Lorenzo et al., 2018; Watanabe et al., 2015). This behavior makes the study of this material of great interest, since higher temperature peaks are normally more stable at room temperature than lower temperature ones, and because it is possible the monitoring of the deposited gamma radiation thought the intensity of the dosimetric TL peak. This paper concerns synthetic undoped $CaSiO_3$ polycrystals exposed in a mixed radiation field (neutron and non-neutron radiation) from the research reactor IEA-R1 of the Institute for Energy and Nuclear Researches of São Paulo (IPEN in its Portuguese acronym). The deposited dose of neutrons from the IAE-R1 reactor on the $CaSiO_3$ polycrystals was achieved through Monte Carlo simulations run with MCNP5 radiation transport code. In addition, $CaSiO_3$ was exposed to ultra-high gamma radiation (Co-60 source) from 500 Gy to 1.2 MGy.

2. Material and methods

2.1. Synthesis

The synthesis process to produce undoped $CaSiO_3$ polycrystals has been explained in a work done previously (Gonzales-Lorenzo et al., 2018). For this purpose, stoichiometric quantities of reagent grade CaO (12.0 g, 48.3 wt%) and SiO_2 (12.8 g, 51.7 wt%) were mixed and then placed in an oven heated to 1500 °C to melt this mixture for 2 h and then cooled slowly. The cooling process was performed with a temperature controller so that after 24 h, room temperature is achieved.

2.2. TL measurements

Polycrystals of $CaSiO_3$ were crushed and sieved to retain grains 80–180 μm in size for gamma and neutron irradiation, and after that, for TL measurements. TL was recorded using Harshaw TL reader model 4500 in a nitrogen atmosphere; heating rate was kept at 4 °C/s. Five TL readings were taken to obtain an average TL glow curve. All TL readings were taken 24 h after irradiation took place. This time period is enough to reach stability of the TL peaks in $CaSiO_3$ polycrystals.

2.3. Gamma irradiation

Irradiations of $CaSiO_3$ samples (in powder form) for high doses in the region of hundreds of Gy up to 50 kGy were carried out at the Radiations Technology Center (CTR) of IPEN using a ^{60}Co source type gamma-cell with a dose rate of 0.64 kGy/h. For ultra-high doses in the region of kGy and MGy (from 70 kGy to 1.2 MGy), samples were irradiated with a ^{60}Co gamma beam from the gamma-cell irradiator at the Nuclear Energy Department of the Federal University of Pernambuco (UFPE), Brazil, operating at 2.571 kGy/h (at the time of irradiation). γ-irradiations at both institutions were performed at room temperature.

2.4. Neutron irradiation

The research reactor IEA-R1 belonging to IPEN São Paulo is a swimming pool-type reactor operating at 5 MW power and has 144 irradiation positions in the core, distributed in 15 irradiation elements for long irradiations and a pneumatic system for short irradiations (up to 5 min). Nine horizontal beam tubes (Beam Holes) that provide neutron beams are also available, used in nuclear physics experiments. Thermal neutrons are considered those with energy < 0.625 eV, for epithermal neutron between 0.625 eV–0.5 MeV, and for fast neutron between 0.5 MeV - 10 MeV. These neutron energy ranges were assessed through the spatial and energetic flux distribution in the IEA R1 reactor core obtained by multiple foil activation technique. Neutron energy spectra were determined by an analysis of the experimental activation data via SAND II (Spectrum Analysis by Neutron Detectors) code (D'utra bitelli, 1988).

$CaSiO_3$ polycrystals in grains selected between 0.080 and 0.180 mm sizes were used in this process as mentioned previously. Seven samples of each about 80 mg were prepared. Each of the samples was sealed in silica tubes each of about 4 mm diameter and 20 mm long. Then, each such tube was placed inside a somewhat larger aluminum tube to be irradiated in a 13 B position in the reactor core. Fig. 1 shows the silica tubes with the samples of $CaSiO_3$ inside as well as the aluminum tube used for irradiation in the reactor. For technical reasons, irradiation was carried out in two different shelf positions (1 and 5) inside the 13 B position (irradiation element). Fig. 2 shows the scheme of the reactor core where the position 13 B can be identified outside the active core area. The time of irradiation, in the shelf position 1 and 5, was programmed in different periods. In the shelf 1, the detectors were irradiated in 5 periods: 60 ± 30, 180 ± 30, 300 ± 30, 600 ± 30 and 240 ± 30 s; whilst for shelf 5 in 2 periods: 360 ± 30 and 5400 ± 108 s. Table 1 shows the neutron fluxes for thermal,

Fig. 1. Silica and aluminum tubes used during the irradiation of the $CaSiO_3$ samples in the IEA-R1 reactor.

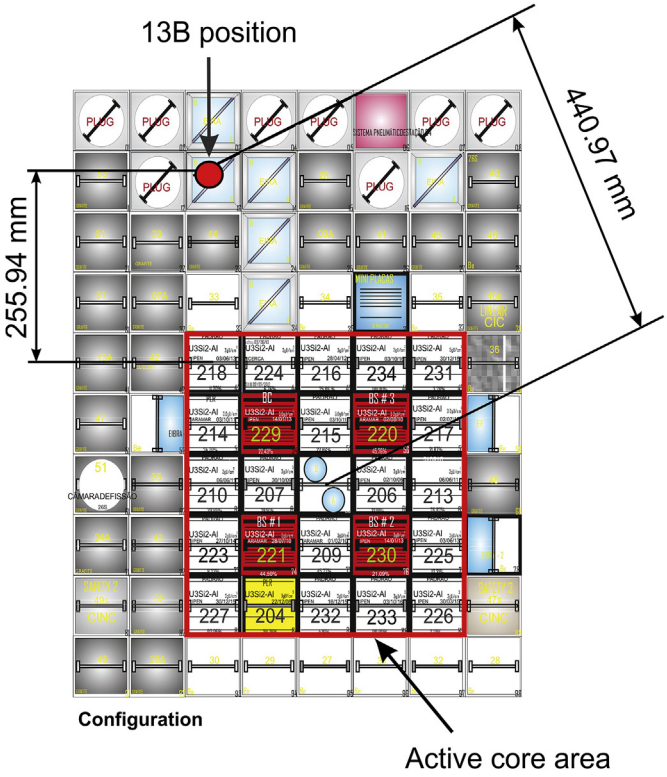

Fig. 2. Reactor core scheme displaying the irradiation position, 13 B, outside the active core area.

epithermal and fast neutrons during the irradiation of samples. Neutron fluxes were measured through the gold foil activation method. Neutron fluxes were measured through the foil activation method. Thermal and epithermal fluxes were assessed by measuring the activities induced on Au foils, with a mass of 1 mg and 2 mm in diameter, using the Westcott formalism. The activities due to the two groups of neutrons were obtained by the cadmium difference method, irradiating two identical gold foils, one of which covered by a cadmium sheet with 0.5 mm of thickness. The fast neutron flux was attained with threshold detectors (^{27}Al, ^{56}Fe, ^{58}Ni) foils. The saturation activities were measured with a high-purity Ge (HPGe) detector with relative gamma detection efficiency previously calibrated with twelve standard radioactive sources to cover the energy range of 150 keV–2400 keV. More details can be found elsewhere. (Koskinas, 1978).

2.5. MCNP5 simulation

The MCNP – A General N-Particle Transport Code, Version 5, was used to find the calculated deposited dose for thermal, epithermal and fast neutrons (X-5 Monte Carlo Team, 2003). ENDF/B-VI.6- and MCPLIB-0- MCNP libraries for neutron and photon transport were used. Geometry: the simulation was carried out considering an aluminum housing (aluminum tube) with 1.095 and 1.030 cm of external and internal radius respectively, and a height of 5.7 cm. In addition, a glass tube was simulated with 0.3 and 0.2 cm of external and internal radius roughly, and with a height of 2.1 cm. The density of aluminum and the glass considering were 2.689 g/cm^3 and 2.400 g/cm^3, respectively. The tallies used were *F4 together with FM to obtain the deposited energy due to the (n,γ) reaction with neutrons of different energy bands. Furthermore, approximately 8 × 10^7 stories were performed per simulation.

3. Results and discussion

The X-ray diffractogram of undoped $CaSiO_3$ polycrystal was presented in our previous work (Gonzales-Lorenzo et al., 2018). It shows all peaks belonging to wollastonite-2M. Although no research has been able to measure neutron and non-neutron effects separately from the TL glow curves of these detectors subjected to a mixed radiation field, it is possible to obtain a clear correspondence between some TL glow curve peaks and neutron fluence, which is a kind of curve calibration. $CaSiO_3$ polycrystals were irradiated with thermal being the largest portion, epithermal in a smaller portion and fast neutrons in a very small fraction as shown in Table 1. Since thermal and epithermal neutrons interact with Ca, Si and O through (n,γ) reaction and as out coming γ induces TL in the dosimeters, the measured effect comes essentially from thermal and epithermal effects (Attix et al., 1969; Glasstone et al., 1981). In a nuclear reactor, few reactions of fast neutrons with atomic nuclei, except scattering and fission, are important. However, the (n,p) reaction may be mentioned which is produced when fast neutrons are captured by ^{16}O (Glasstone et al., 1981).

3.1. TL results

First of all, samples of $CaSiO_3$ in grains (80–180 μm diameter) were irradiated with different gamma-doses. Fig. 3 (a) shows TL glow curves of the $CaSiO_3$ irradiated with gamma doses from 500 Gy to 1.2 MGy. For gamma irradiation dose from 500 Gy to 1 kGy the TL peak at about 272 °C is prominent. However, for gamma irradiation dose of 7 kGy to 1.2 MGy the prominent TL peak is that at about 234 °C. In the same way as gamma irradiation, for thermal neutron fluence from 1.75 × 10^{14} to 2.91 × 10^{14} the TL peak at about 234 °C is prominent. Fig. 3 (b) shows the TL glow curves of the undoped $CaSiO_3$ for different thermal neutron fluences from 5.82 × 10^{13} to 2.97 × 10^{16} n/cm^2.

Fig. 4 shows the TL response of the main TL peak (around at 234 °C) as a function of gamma dose (blue circle). It can be observed that the TL response has a supralinear behavior up to 7 kGy and then it saturates, after that, TL response decreases slowly with the increase in dose from 50 kGy to 1.2 MGy. On the other hand, the curve in red (red triangle) shows the response of the main TL peak (around at 234 °C) after reactor exposure, as a function of thermal neutron fluences ranging from 5.82 × 10^{13} to 2.97 × 10^{16} n/cm^2. This curve has a growing non-linear behavior, from 5.82 × 10^{13} to 1.98 × 10^{15} n/cm^2 thermal neutron fluence. Consequently, it can be proposed that TL response for neutron irradiation can go into saturation to thermal neutron fluences greater than of 1.98 × 10^{15} n/cm^2 and then slowly decreasing in intensity, in the same way as gamma dose irradiation. Moreover, it can be observed in Fig. 4 that the TL response higher than 2.91 × 10^{14} n/cm^2 fluences is lesser than the TL responses for high-gamma radiation. This may be due to the radiation damage effect on the sample when it is exposed to ultra-high neutron radiation (higher than 2.91 × 10^{14} n/cm^2) but this effect requires supplementary studies. Piesch et al. (1978) and Gambarini et al. (2004) have observed that LiF dosimeters when exposed to high fluences of thermal neutrons lose linearity and undergo radiation damage. For this reason, Gambarini et al. (2004) proposed a rough

Table 1
Neutron fluxes during irradiation at the IEA-R1nuclear reactor.

Position	Shelf Position	Thermal flux (n/s•cm^2)	Epithermal flux (n/s•cm^2)	Fast flux (n/s•cm^2)
13 B	1	(9.70 ± 0.26) x10^{11}	(1.13 ± 0.03) x10^{11}	(9.39 ± 0.25) x10^{10}
13 B	5	(5.50 ± 0.15) x10^{12}	(7.33 ± 0.20) x10^{11}	(3.99 ± 0.11) x10^{11}

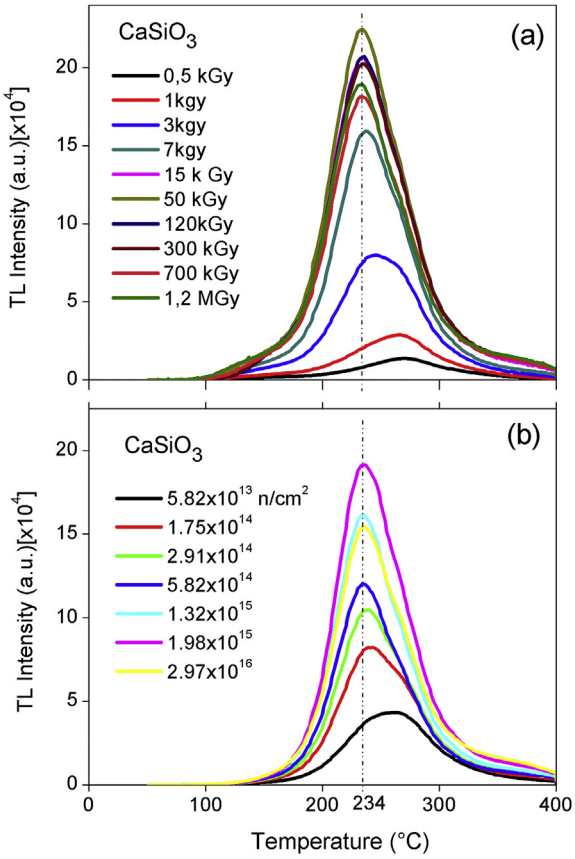

Fig. 3. (a) TL glow curves of $CaSiO_3$ irradiated with high and ultra-high gamma dose from 500 Gy to 1.2 MGy, (b) TL glow curve of $CaSiO_3$ irradiation with different thermal fluences from 5.82 × 10^{13} to 2.97 × 10^{16} n/cm^2.

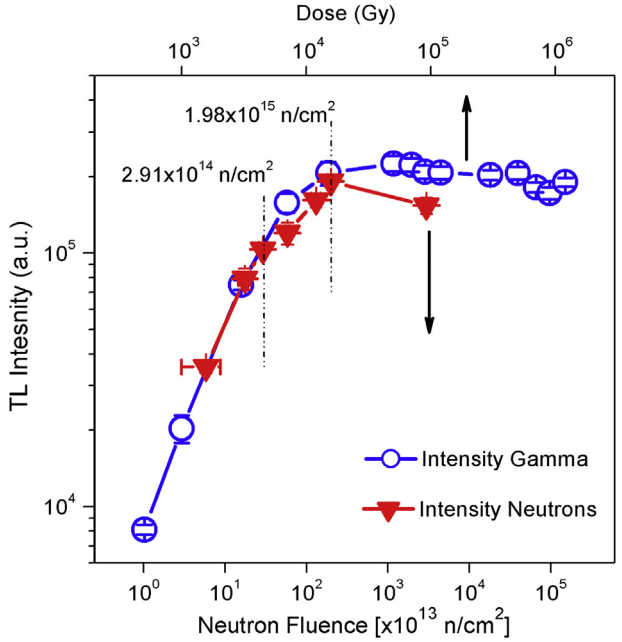

Fig. 4. TL intensity behavior of the main peak at about 234 °C as a function of gamma doses (○ blue circle) and the TL intensity of the main peak at about 234 °C as a function of thermal neutron fluence (Δ red triangle). (For interpretation of the references to colour in this figure legend, the reader is referred to the Web version of this article.)

correction of the results by means of re-calibrating the dosimeters through gamma radiation after neutron irradiation.

Additionally, it can be observed in Fig. 4 that the TL responses lower than 2.91 × 10^{14} n/cm^2 is similar to those irradiated with gamma radiation lower than 4 kGy. In this way, taking advantage of this behavior it is possible to calculate the absorbed gamma dose by the $CaSiO_3$ after reactor irradiation. That is, after reactor exposure, the nuclear reactor enters a state of interruption where no neutron fluxes are emitted but gamma radiation continues to be emitted through the active core of the reactor. For this reason, we make a linear extrapolation of the TL response lower than 2.91 × 10^{14} n/cm^2. In this way, for a thermal neutron fluence value of zero, we have a TL intensity of about 1.38 × 10^4 a.u. On the other hand, for gamma radiation dose the TL response is supralinear from a few hundreds of Gy to 7 kGy as mentioned above. Thus, for a TL intensity of 1.38 × 10^4 a.u. (neutron extrapolation), we have, using the supralinear extrapolation for gamma radiation dose, a value of gamma dose of about 730 Gy. This result shows us that the amount of absorbed gamma dose by the material after the neutrons flux ceases at the point of irradiation 13 B (shelf 1) is about 730 Gy. This result is of interest for the IEA-R1 reactor, because no residual gamma irradiation dose has been calculated up to now.

3.2. The (n,γ) reaction for Ca, Si and O

The interaction of the thermal neutrons from the research reactor IEA-R1 with polycrystalline calcium silicate has been analyzed analytically in this section. In the irradiation of $CaSiO_3$ with thermal neutrons, the mai1n effect is the (n,γ) reaction that takes place with Ca, Si and O. For this reason, the energy of γ-rays emitted when a thermal neutron is absorbed by each element of the $CaSiO_3$ has been calculated ((n,γ) reaction). Since each element can exist in different types, called isotopes, we need to consider the natural abundance of the isotopes of each element studied. We shall consider ^{40}Ca, ^{28}Si, and ^{16}O, the most abundant isotopes, in accordance with Meija et al. (2016).

The capture of the thermal neutron (slow neutron) by a nucleus results in the release of a large amount of energy. The energy that is released in this reaction is called the binding energy of a neutron in the particular nucleus formed. The Q-value of a nuclear reaction is the measure of the energy "released" or "absorbed" by the reaction. It is calculated by the difference between the sum of the masses of the initial reactants and the sum of the masses of the final products, in energy units (usually in MeV) (Magill and Galy, 2005). In this case, for the ^{40}Ca (n,γ)^{41}Ca reaction, the Q value is expressed as Q (Ca) = $M_0(^{40}Ca)$ •c^2 + M_0(n)•c^2 − $M_0(^{41}Ca)$•c^2; where $M_0(^{40}Ca)$ is the atomic mass of ^{40}Ca and $M_0(^{41}Ca)$ is the atomic mass of ^{41}Ca. We shall consider the most abundant isotope of calcium, the ^{40}Ca with an abundance (in amount fraction) of 0.969 41(156) and an atomic mass of 39.962 5909 u (Meija et al., 2016). The atomic mass for ^{41}Ca, $M_0(^{41}Ca)$ is 40.96227806(26) (Sukhoruchkin and Soroko, 2009). M_0(n) is the relative atomic mass of the neutron equal to 1.008 664 915 74(56) u (Mohr et al., 2010). Thus, using the equation for Q mentioned earlier, we obtain, Q(Ca) ≈ 8362.73 keV which is in good agreement with Gruppelaar and Spilling (1967). Gruppelaar and Spilling (1967) with the help of the least-squares program have calculated a more accurate Q-value for the ^{40}Ca(n,γ)^{41}Ca reaction as Q = 8363.4 keV with a statistical error of 1.0 keV. This Q-value was calculated considering the decay scheme of ^{41}Ca in which cascades between the capturing state and the ground state were selected with the aid of a computer program. In the same way as Ca, considering the isotopic abundance of Si as well as the atomic mass of ^{28}Si and ^{29}Si for the ^{28}Si(n,γ)^{29}Si reaction (Meija et al., 2016), the calculated Q-value is Q(Si) ≈ 8473.60 keV which is in good agreement with Spits et al. (1970). For the ^{16}O(n,γ)^{17}O reaction, considering the isotopic abundance of O and the values of the atomic mass of ^{16}O and ^{17}O (Meija et al., 2016), the calculated Q-value is Q (O) ≈ 4143.08 keV which is in good agreement with Firestone et al. (2004). Spits et al. (1970) and Firestone et al. (2004) have calculated

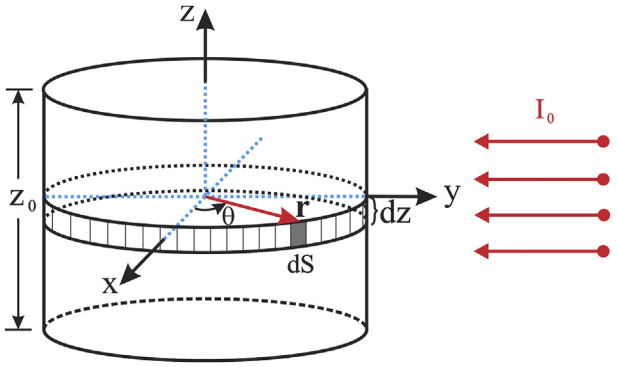

Fig. 5. Scheme of the sample irradiation in a cylindrical coordinate disposition.

more accurate Q-values for $^{28}Si(n,\gamma)^{29}Si$ and $^{16}O(n,\gamma)^{17}O$ reactions as Q(Si) = 8473.5 ± 0.5 keV and Q(O) = 4143.06 ± 0.10 keV respectively.

3.3. Neutron absorption

The results of the calculation of the total thermal neutrons absorbed on the sample of $CaSiO_3$ is presented in this section. For this purpose, a sample of $CaSiO_3$ in grains, inside a cylindrical geometry tube (silica tube) has been considered. Total neutron absorption N at a distance *x* from the sample can be expressed by equation $N(x) = N(0)\cdot\exp(-\upsilon x)$ (Van Eijk, 2004), where N(*x*) and N(0) are the neutron fluence at a depth *x* in the material and before entering the material respectively. υ is the linear absorption coefficient (cm^{-1}): $\upsilon = N_A\cdot\rho\cdot\sigma_A\cdot\omega/A$. N_A is Avogadro's number, ρ is the sample density, σ_A is the energy-dependent capture cross-section for each element, A is the atomic mass and ω is the weight fraction of each element in the material. σ_A for thermal neutrons capture is called thermal cross-section. For ^{40}Ca, the thermal cross-section is 0.41 ± 0.02 b, for ^{28}Si is 0.177 ± 0.004 b, and for ^{16}O is 190 ± 0.019 mb. These values were obtained from the book: Atlas of Neutron Resonances and Thermal Cross Section (Mughabghab, 2006).

Fig. 5 shows the cylindrical disposition of the sample of $CaSiO_3$ during neutron exposure. For calculation purposes, the effect of the silica and aluminum tube, as well as the particle size of the sample in neutron irradiations were not considered. The total thermal neutrons absorbed n_{abs} by each element on the sample were calculated using equation (1) which was calculated analytically and considering the cylindrical disposition of the sample.

$$n_{abs} = I_0\cdot t\cdot r\cdot z_0\left(\pi - \int_0^{\pi} e^{-2N\sigma r\,\mathrm{sen}\theta}d\theta\right) \quad (1)$$

Where I_0 is the initial neutron flux in $n/cm^2\cdot s$, t is the irradiation time of the flux on the sample, r is the radius of the transverse circumference of the silica tube and z_0 is the height of the sample inside the silica tube (2r = 4 ± 0.05 mm, z_0 = 6 ± 0.05 mm). $N = \rho\cdot N_A\cdot\omega/A$, ρ ≈ 1.47 g/$cm^3$ and θ is the azimuthal angle in a cylindrical coordinate disposition as shown in Fig. 5. Therefore, for a thermal fluence of (29.1 ± 3.0) $x10^{13}$ n/cm^2 the total thermal neutrons absorbed n_{abs} by each element on the sample is: $n_{abs}(Ca) = (919 \pm 96)x10^8$; $n_{abs}(Si) = (603 \pm 63)$ $x10^7$; and $n_{abs}(O) = (118 \pm 12)x10^9$ neutrons. Finally, with the above considerations, the total energy released or total Q-value of all the nuclear reactions produced on the sample during thermal neutron irradiation was obtained. The total energy released at a given fluence (f) is calculated using equation (2).

$$Q_f(CaSiO_3) = n_{f,\,abs}(Ca)\cdot Q(Ca) + n_{f,\,abs}(Si)\cdot Q(Si) + n_{f,\,abs}(O)\cdot Q(O) \quad (2)$$

Table 2 shows the total energy released at different thermal neutron fluences. The Q-values used in this calculation were taken from Gruppelaar and Spilling (1967), Spits et al. (1970) and Firestone et al. (2004).

Table 2
Total released energy calculated on the sample of $CaSiO_3$ at each thermal neutron fluence.

Thermal neutron fluences (n/cm^2) [$x10^{13}$]	Total released energy (MeV) [$x10^{11}$]
5.82 ± 2.91	2.62 ± 0.90
17.5 ± 2.95	7.87 ± 0.93
29.1 ± 3.0	13.1 ± 1.0
58.2 ± 3.3	26.2 ± 1.1
132 ± 17	59.3 ± 5.4
198 ± 17	89.0 ± 5.4
2970 ± 100	1330 ± 34

3.4. Deposited dose calculation

Not all energies released in the sample of $CaSiO_3$ during neutron irradiation by the nuclear reactions are absorbed. Only a small portion will contribute to the total deposited dose. In (n,γ) reactions for Ca, Si and O, the excited compound nucleus, after neutron capture, emits its excess energy as gamma radiation leaving the nucleus in the lowest energy state. This energy emitted is about 8.36 MeV for Ca, 8.47 MeV for Si and about 4.14 MeV for O, as shown earlier. Usually, this excess energy is emitted as several photons from kGy to MeV (Glasstone et al., 1981; Firestone and Shirley, 1996). Part or all of the energy emitted can be absorbed, or may even reach other elements on the sample, in its trajectory. In this case, several other kinds of processes may appear where photon interaction is involved (Attix, 2008). In addition, taking into account that the sample is small of the order of mm^3, it allows the γ radiation of high intensity to escape (Attix et al., 1969). For this purpose, the calculation of the deposited dose on the sample of $CaSiO_3$ after the neutron irradiation was carried out using the MCNP5 code. This code takes into account the neutron energy either, thermal, epithermal or fast neutrons during the neutron interaction with the polycrystal. Also, the simulation was considered the real geometrical disposition and the sample of $CaSiO_3$ located inside the silica tube and it, in turn, located inside the aluminum tube as explained before. All neutrons (thermal, epithermal and fast neutrons) before reaching the sample interacts with aluminum (first) and silica tube (second) through different processes mainly through the (n,γ) reaction producing the emission of photons. These photons produced together with the photons emitted in the interaction of neutrons with the sample which was not initially absorbed, subsequently may be absorbed by the sample. Al and Si having a low cross-section for thermal neutrons capture of the order of mb (Mughabghab, 2006). The deposited dose due to those absorbed photons was also calculated by Monte Carlo code and added to the total deposited dose. It is important to mention that the processes related to the gamma rays produced in the reactor were not considered in the calculations due to the lack of experimental data on both spatial and energetic distribution, neither for prompt photons nor for those from decays of fission products. However, all neutron irradiation on the sample was considered.

In addition to the above, it is possible to calculate the energy absorbed by the material from the calculated deposited dose using the mass of polycrystals of $CaSiO_3$ (sample) used during neutron irradiation and the conversion factor 1 MeV/1 kg = 1.6021×10^{-13} Gy (Attix et al., 1969). The mass used in each sample was about ≈110 mg. Table 3 shows the calculated deposited dose and the calculated energy absorbed due to neutron interaction with this sample of $CaSiO_3$ for each thermal neutron fluence through the Monte Carlo simulation. Thereby, it is possible to make a comparison between the results shown in Tables 2 and 3 That is, the calculated released energy through the (n,γ) reaction and the calculated absorbed energy through the Monte Carlo

Table 3
Calculated deposited dose and calculated absorbed energy in a sample of $CaSiO_3$ (mass ≈ 110 mg) at each thermal neutron fluence.

Thermal neutron fluences (n/cm^2) [x10^{13}]	Deposited dose (Gy)	Absorbed energy (MeV) [x10^9]
5.82 ± 2.91	41.5 ± 0.2	28.5 ± 0.1
17.5 ± 2.95	125 ± 1	85.5 ± 0.4
29.1 ± 3.0	208 ± 1	143 ± 1
58.2 ± 3.3	415 ± 2	285 ± 1
132 ± 17	935 ± 5	642 ± 3
198 ± 17	1400 ± 7	963 ± 5
2970 ± 100	21000 ± 103	1450 ± 70

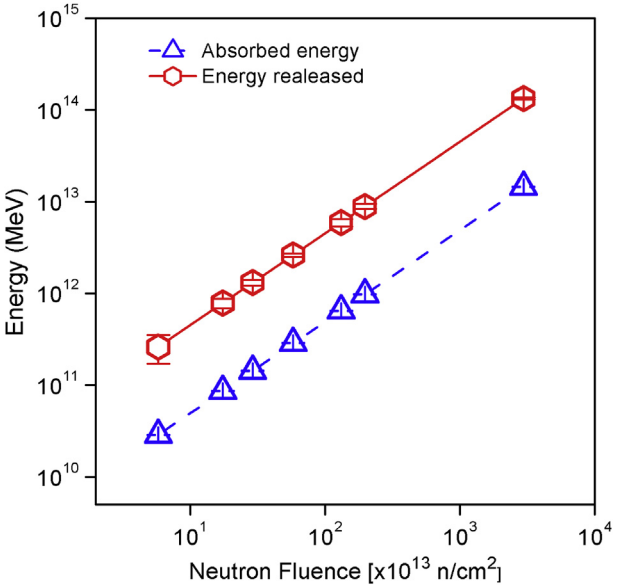

Fig. 6. The calculated released energy and the calculated absorbed energy after thermal neutron irradiation on the sample of $CaSiO_3$ as a function of thermal neutron fluence.

method after the thermal neutron irradiation on the polycrystal of $CaSiO_3$. A comparison between these results as a function of thermal neutron fluence is shown in Fig. 6.

4. Conclusions

In this study, polycrystalline $CaSiO_3$ has been synthesized using the devitrification method. The results showed the same TL glow curve behavior after reactor exposure (neutron + non-neutron radiation) and gamma radiation (from Co-60 source) with the main TL peak at about 234 °C. The curve of the TL intensity of the main peak vs. the neutron fluence, after reactor exposure, shows a growing non-linear behavior similar to that with gamma irradiation up to a thermal fluence of 1.98×10^{15} n/cm^2. In this way, polycrystals of $CaSiO_3$ are sensitive to neutron radiation from the nuclear reactor, however, a supplementary study will be performed in order to know the radiation damage effect produced in the polycrystal for thermal neutron fluences higher than 2.91×10^{14} n/cm^2.

Furthermore, a comparison between the curve-response of the $CaSiO_3$ sample after gamma and reactor irradiation show that these curves have similar behavior for thermal neutron fluences lower than 2.91×10^{14} n/cm^2 and for gamma dose irradiation lower than 4 kGy.

The absorbed gamma dose by the $CaSiO_3$ after neutron exposure was calculated by extrapolation of the TL response lower than 2.91×10^{14} n/cm^2 of thermal neutron fluence and extrapolation of TL response lower than 4 kGy of gamma radiation dose. It was found that the amount of absorbed gamma dose by this sample after the neutrons flux ceases at the point of irradiation 13 B (shelf 1) is about 730 Gy.

An approximation of the total released energy during the interaction of the thermal neutron with the sample in the position of irradiation was calculated ranging from about 2.62×10^{11} for a thermal neutron fluence of 5.82×10^{13} n/cm^2 to 1.33×10^{14} MeV for a thermal neutron fluence of 2.97×10^{16} n/cm^2. Additionally, the Monte Carlo calculation of the deposited dose varies from 42 Gy for a thermal neutron fluence of 5.82×10^{13} n/cm^2 to 21 kGy for a thermal neutron fluence of 2.97×10^{16} n/cm^2.

The comparison shown in Fig. 6 between the total released energy calculated analytically through the (n,γ) reaction during the thermal neutron irradiation and Monte Carlo calculation of the absorbed energy shows that about 11% of the total released energy is absorbed by the sample of $CaSiO_3$ with a mass of about 110 mg.

We are carrying out the study of $CaSiO_3$ polycrystalline doped with different quantities in ppm of Eu keeping in mind the high cross-section for thermal neutron capture of this element. We expect to have a more sensitive material than undoped $CaSiO_3$ for thermal neutrons radiation.

CRediT authorship contribution statement

Carlos D. Gonzales-Lorenzo: Conceptualization, Methodology, Investigation. **Shigueo Watanabe:** Supervision, Project administration, Funding acquisition. **Tássio A. Cavalieri:** Methodology, Software, Data curation. **Nilo F. Cano:** Project administration, Formal analysis. **T.K. Gundu Rao:** Writing - original draft, Visualization. **Jose F.D. Chubaci:** Writing - review & editing, Resources. **Lucas S. Carmo:** Methodology, Validation. **Carmen C. Bueno:** Resources, Investigation, Supervision.

Declaration of competing interest

The authors declare that they have no known competing financial interests or personal relationships that could have appeared to influence the work reported in this paper.

Acknowledgments

The authors wish to thank Ms. E. Somessari and Mr. Aldo Oliveira from the Institute for Energy and Nuclear Researches (IPEN), Brazil, and Dr. H. Khoury from the Nuclear Energy Department of the Federal University of Pernambuco, Brazil, for kindly carrying out the irradiation of the samples. To Dr. M.F. Koskinas and Dr. M.S. Dias, both from IPEN, for helpful discussions on the neutron activation method and the measurements of the neutron fluxes in the IEA-R1 reactor. This work was carried out with partial financial support from Fundação de Amparo à Pesquisa do Estado de São Paulo - FAPESP, Brazil (Process number 2014/03085-0). To Consejo Nacional de Desarrollo Científico y Tecnológico - CNPq, Brazil, for fellowship to C.D. Gonzales-Lorenzo (Process number 162741/2015-4).

References

Attix, F.H., Roesch, W.C., Tochilin, E., 1969. Radiation Dosimetry. Academic Press, New York.
Attix, F.H., 2008. Introduction to Radiological Physics and Radiation Dosimetry. John Wiley & Sons, USA.
Cameron, J.R., Suntharalingam, N., Kenney, G.N., 1968. Thermoluminescent Dosimetry. University of Wisconsin Press, Madison.
Carrillo, R.E., Uribe, R.M., Woodruff, G.L., Stoebe, T.G., 1987. Lithium fluoride (TLD-700) response to a mixed thermal neutron and gamma field. Radiat. Protect. Dosim. 19, 55–57. https://doi.org/10.1093/oxfordjournals.rpd.a079920.
Cavalieri, T.A., Castro, V.A., Siqueira, P.T.D., 2013. Differences in TLD 600 and TLD 700 glow curves derived from distict mixed gamma/neutron field irradiations. In: INAC 2013: International Nuclear Atlantic Conference, pp. 24–29 Brazil.
Cavalieri, T.A., Siqueira, P.T.D., Shorto, J.M.B., Genezini, F.A., Yoriyaz, H., 2019. Design, fabrication and modeling of an AmBe neutron irradiator for TLD screening for neutron dose measurement in mixed radiation fields. Appl. Radiat. Isot. 150, 31–38. https://doi.org/10.1016/j.apradiso.2019.05.009.
Cerón Ramírez, P.V., Díaz Góngora, J.A., Paredes Gutiérrez, L.C., Rivera Montalvo, T., Vega Carrillo, H.R., 2016. Neutron H*(10) estimation and measurements around

18MV linac. Appl. Radiat. Isot. 117, 2–7. https://doi.org/10.1016/j.apradiso.2016.05.006.
Deer, W.A., Howie, R.A., Zussman, J., 1992. An Introduction to the Rock-Forming Minerals, second ed. Longman, England.
Douglas, J.A., 1978. The Applications of TL Materials in Neutron Dosimetry. UKAEA, Harwell. Atom. Ener. Res. Establ., United Kingdom.
D'utra bitelli, U., 1988. Medida e cálculo da distribuição espacial e energética de nêutrons no núcleo do reator IEA-R1. Unpublished master's thesis. Institute for Energy and Nuclear Researches, São Paulo.
Fernandes, A.C., Santos, J.P., Kling, A., Marques, J.G., Gonçalves, I.C., Carvalho, A.F., Santos, L., Cardoso, J., Osvay, M., 2004. Thermoluminescence dosimetry of a thermal neutron field and comparison with Monte Carlo calculations. Radiat. Protect. Dosim. 111, 35–39. https://doi.org/10.1093/rpd/nch356.
Firestone, R.B., Shirley, V.S., 1996. Table of Isotopes, eighth ed. John Wiley.
Firestone, R.B., Choi, H.D., Lindstrom, R.M., 2004. Database of Prompt Gamma Rays from Slow Neutron Capture for Elemental Analysis. LBNL, Berkeley Technical Report.
Gambarini, G., Klamert, V., Agosteo, S., Birattari, C., Gay, S., Rosi, G., Scolari, L., 2004. Study of a method based on TLD detectors for in-phantom dosimetry in BNCT. Radiat. Protect. Dosim. 110, 631–636. https://doi.org/10.1093/rpd/nch109.
Glasstone, S., Sesonske, A., United States Dept of Energy, 1981. Nuclear Reactor Engineering, third ed. Van Nostrand Reinhold, New York.
Gonzales-Lorenzo, C.D., Watanabe, S., Cano, N.F., Ayala-Arenas, J.S., Bueno, C.C., 2018. Synthetic polycrystals of $CaSiO_3$ un-doped and Cd, B, Dy, Eu-doped for gamma and neutron detection. J. Lumin. 201, 5–10. https://doi.org/10.1016/j.jlumin.2018.04.037.
Gruppelaar, H., Spilling, P., 1967. Thermal-neutron capture gamma rays from natural calcium. Nucl. Phys. A 102, 226–236. https://doi.org/10.1016/0375-9474(67)90333-8.
Hesse, K., 1984. Refinement of the crystal structure of wollastonite-2M (para-wollastonite). Z. Kristallogr. 168, 93–98. https://doi.org/10.1524/zkri.1984.168.14.93.
Kortov, V., Ustyantsev, Y., 2013. Advantages and challenges of high-dose thermo-luminescent detectors. Radiat. Meas. 56, 299–302. https://doi.org/10.1016/j.radmeas.2013.03.018.
Koskinas, M.F., 1978. Medidas De Fluxo De Neutrons Térmicos, Epitérmicos E Rápidos No Reator IEA-R1, Pela Técnica De Ativação De Folhas. Unpublished master's thesis. Institute for Energy and Nuclear Researches, São Paulo.
Kulkarni, S., Nagabhushana, B.M., Nagabhushana, H., Murthy, K.V.R., Shivakumara, C., Damle, R., 2011. Synthesis, structural characterization and thermoluminescence properties of β-irradiated wollastonite nanophosphor. Trans. Indian Ceram. Soc. 70, 163–166. https://doi.org/10.1080/0371750X.2011.10600165.
Magill, J., Galy, J., 2005. Radioactivity Radionuclides Radiation. Springer Science & Business Media.
Meija, J., Coplen, T.B., Berglund, M., Bran, W.A., De Bièvre, P., Gröning, M., Holden, N.E., Irrgeher, J., Loss, R.D., Walczyk, T., 2016. Isotopic compositions of the elements 2013 (IUPAC technical report). Pure Appl. Chem. 88, 293–306. https://doi.org/10.1515/pac-2015-0503.
Mohr, P.J., Taylor, B.N., Newell, D.B., 2010. Codata recommended values of the fundamental physical constants: 2010. Rev. Mod. Phys. 84, 1527–1605. https://doi.org/10.1103/RevModPhys.84.1527.
Mughabghab, S.F., 2006. fifth ed. Atlas of Neutron Resonances: Resonance Parameters and Thermal Cross Sections, Z = vols. 1–100 Elsevier, Amsterdam.
Obryk, B., Glaser, M., Mandić, I., Bilski, P., Olko, P., Sas-Bieniarz, A., 2011. Response of various types of lithium fluoride MCP detectors to high and ultra-high thermal neutron doses. Radiat. Meas. 46, 1882–1885. https://doi.org/10.1016/j.radmeas.2011.06.050.
Obryk, B., Malik, K., Bilski, P., Igielski, A., Dankowski, J., Kurowski, A., Prokopowicz, R., Pytel, K., 2018. High-dose TL dosimetry of reactor neutrons. Radiat. Protect. Dosim. 180, 235–239. https://doi.org/10.1093/rpd/ncx244.
Piesch, E., Burgkhardt, B., Sayed, A.M., 1978. Activation and damage effects in TLD 600 after neutron irradiation. Nucl. Instrum. Methods 157, 179–184. https://doi.org/10.1016/0029-554X(78)90604-3.
Simpsons, R.E., 1965. Response of LiF to reactor neutrons. In: Proceedings of International Conference on Luminescence Dosimetry, pp. 444–456 Stanford.
Souza, D.N., Melo, A.P., Gazano, V.S.O., Caldas, L.V.E., 2006. Characterization of Brazilian Wollastonite for radiation dosimetry. In: Proceedings of the IJM. Acapulco, (Mexico).
Spits, A.M.J., Op Den Kamp, A.M.F., Gruppelaar, H., 1970. Gamma rays from thermal-neutron capture in natural and 28Si enriched silicon. Nucl. Phys. A 145, 449–460. https://doi.org/10.1016/0375-9474(70)90435-5.
Sukhoruchkin, S., Soroko, Z., 2009. Atomic mass and nuclear binding energy for Ca-41 (calcium). In: In: Schopper, H. (Ed.), Nuclei with Z = 1 - 54, vol. 22. Springer, Berlin, Heidelberg, pp. 1434–1436. https://doi.org/10.1007/978-3-540-69945-3_653.
Torres-Cortés, C.O., Hernández-Adame, L., Baltazar-Raigosa, A., Vega-Carrillo, H.R., Rodríguez-López, J.L., Pérez-Arrieta, M.L., 2019. Synthesis and thermoluminescent response to γ-rays and neutrons of MgB_4O_7:Dy and MgB_4O_7:Dy,Na. Appl. Radiat. Isot. 147, 159–164. https://doi.org/10.1016/j.apradiso.2019.03.001.
Van Eijk, C.W.E., 2004. Inorganic scintillators for thermal neutron detection. Radiat. Meas. 38, 337–342. https://doi.org/10.1016/j.radmeas.2004.02.004.
Vega-Carrillo, H.R., 2002. TLD pairs, as thermal neutron detectors in neutron multisphere spectrometry. Radiat. Meas. 35 (3), 251–254. https://doi.org/10.1016/S1350-4487(01)00291-8.
Watanabe, S., Cano, N.F., Carmo, L.S., Barbosa, R.F., Chubaci, J.F.D., 2015. High- and very-high-dose dosimetry using silicate minerals. Radiat. Meas. 72, 66–69. https://doi.org/10.1016/j.radmeas.2014.11.004.
X-5 Monte Carlo Team, 2003. MCNP - A General N-Particle Transport Code. Version 5, vol. 1 Los Alamos National Laboratory, Los Alamos.